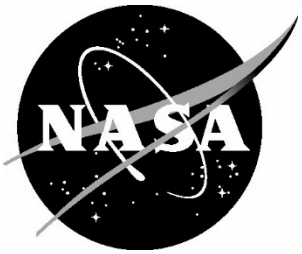
NASA/TM–20240012407



Bumper Implementation of LMEEM

Kevin D. Deighton
Amentum Services, Inc
NASA Johnson Space Center, Houston, TX
Astromaterials Research and Exploration Science

June 2024

NASA STI Program Report Series

Since its founding, NASA has been dedicated to the advancement of aeronautics and space science. The NASA scientific and technical information (STI) program plays a key part in helping NASA maintain this important role.

The NASA STI program operates under the auspices of the Agency Chief Information Officer. It collects, organizes, provides for archiving, and disseminates NASA's STI. The NASA STI program provides access to the NTRS Registered and its public interface, the NASA Technical Reports Server, thus providing one of the largest collections of aeronautical and space science STI in the world. Results are published in both non-NASA channels and by NASA in the NASA STI Report Series, which includes the following report types:

- TECHNICAL PUBLICATION. Reports of completed research or a major significant phase of research that present the results of NASA Programs and include extensive data or theoretical analysis. Includes compilations of significant scientific and technical data and information deemed to be of continuing reference value. NASA counterpart of peer-reviewed formal professional papers but has less stringent limitations on manuscript length and extent of graphic presentations.

- TECHNICAL MEMORANDUM. Scientific and technical findings that are preliminary or of specialized interest, e.g., quick release reports, working papers, and bibliographies that contain minimal annotation. Does not contain extensive analysis.

- CONTRACTOR REPORT. Scientific and technical findings by NASA-sponsored contractors and grantees.

- CONFERENCE PUBLICATION. Collected papers from scientific and technical conferences, symposia, seminars, or other meetings sponsored or co-sponsored by NASA.

- SPECIAL PUBLICATION. Scientific, technical, or historical information from NASA programs, projects, and missions, often concerned with subjects having substantial public interest.

- TECHNICAL TRANSLATION. English-language translations of foreign scientific and technical material pertinent to NASA's mission.

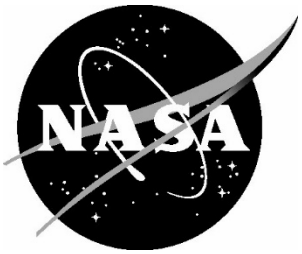
Specialized services also include organizing and publishing research results, distributing specialized research announcements and feeds, providing information desk and personal search support, and enabling data exchange services.

For more information about the NASA STI program, see the following:

- Access the NASA STI program home page at http://www.sti.nasa.gov

.

NASA/TM–20240012407



Bumper Implementation of LMEEM

Kevin D. Deighton
Amentum Services, Inc
NASA Johnson Space Center, Houston, TX
Astromaterials Research and Exploration Science

National Aeronautics and
Space Administration

NASA Johnson Space Center
Houston, TX

June 2024

The use of trademarks or names of manufacturers in this report is for accurate reporting and does not constitute an official endorsement, either expressed or implied, of such products or manufacturers by the National Aeronautics and Space Administration.

Available from:

NASA STI Program / Mail Stop 050
NASA Langley Research Center
Hampton, VA 23681-2199

TABLE OF CONTENTS

TABLE OF CONTENTS v
TABLES vi
FIGURES vii
1. Executive Summary 1
1.1. Acronyms and Abbreviations 1
2. Reading the LMEEM File 2
2.1. Bumper Analysis with LMEEM 4
3. Validation of Bumper Calculations 6
3.1. Basic Intent 6
3.2. Bumper Calculation Process 9
4. Initial LMEEM Environment File 11
4.1. Current & Future LMEEM Features 13
5. Comparison between SP-8013 & LMEEM 14
6. Conclusion 19
7. References 20

TABLES

Table 3-1 Basic Intent Hand Calculation Comparison 9
Table 3-2 Igloo Calculation Hand Calculation Comparison..... 10
Table 3-3 Flux Calculation Hand Calculation Comparison..... 10
Table 5-1 Basic Ejecta Risk Comparison..... 14
Table 5-2 LMEEM Risk by Velocity 15

FIGURES

Figure 2-1 Example LMEEM Environment File Header 2
Figure 2-2 Example LMEEM Environment File Data Block..... 3
Figure 3-1 LMEEM Igloo..... 6
Figure 3-2 Average Azimuth Cosine..... 8
Figure 4-1 LMEEM Flux as a Function of Mass (Compared to SP-8013)..... 11
Figure 4-2 LMEEM Flux Directionality 12
Figure 4-3 LMEEM Flux Ascending vs. Descending..... 13
Figure 5-1 Ejecta Contour Comparison: 6 mm Impacts..... 16
Figure 5-2 Ejecta Contour Comparison: Whipple Shield Penetrations 16

1. Executive Summary

The Hypervelocity Impact Technology (HVIT) group at the NASA Johnson Space Center (JSC) maintains the Bumper 3 computer program (referred to as "Bumper") to perform Micrometeoroid and Orbital Debris (MMOD) risk assessments for spacecraft. To perform its calculations, this program requires detailed mathematical models of the space environments and can include those models representing orbital debris, micrometeoroids, and lunar ejecta.

The lunar ejecta environment is a projectile environment specific to the lunar surface. Due to the Moon's lack of an atmosphere, meteoroids frequently strike the lunar surface. When this happens, the impact ejects material radially away from the impact point, which can pose a potential impact hazard to surface-based hardware.

This lunar ejecta environment was previously described in 1969, in NASA Special Publication SP-8013 [1], which was used as the basis for a model that will be referred to in this document as the "SP-8013 environment model," or simply, "SP-8013." Since around 2020, this model has been used in MMOD risk assessments for the Human Landing System (HLS) program and other lunar surface programs.

A new lunar meteoroid ejecta environment was developed via a computer code named Lunar Meteoroid Ejecta Engineering Model (LMEEM), produced by the Natural Environments Branch (NEB) at Marshall Space Flight Center (MSFC). A global lunar surface environment definition using LMEEM is to be provided in the Cross-Program Design Specification for Natural Environments (DSNE) Revision J in 2024. Contact the NASA MSFC Natural Environments Branch for an in-depth discussion of the LMEEM environment model and its derivation. This environment model will supersede SP-8013 for MMOD risk assessments.

To perform such assessments, Bumper must read data from text files output by LMEEM and use that data in risk calculations. The purpose of this document is to:

- Demonstrate verification that the Bumper code has properly implemented the LMEEM environment model (Section 3)
- Discuss the LMEEM environment as understood through an initial environment file (Section 4)
- Compare the calculated risk due to the SP-8013 and LMEEM models (Section 5)

1.1. Acronyms and Abbreviations

ASCII	American Standard Code for Information Interchange
BLE	Ballistic Limit Equation
DSNE	Design Specification for Natural Environments
FEM	Finite Element Model
HLS	Human Landing System
HVIT	Hypervelocity Impact Technology (group)
JSC	Johnson Space Center
LMEEM	Lunar Meteoroid Ejecta Engineering Model
MEM	Meteoroid Engineering Model
MEO	Meteoroid Environment Office
MMOD	Micrometeoroid and Orbital Debris
MSFC	Marshall Space Flight Center
NASA	National Aeronautics and Space Administration
NEB	Natural Environments Branch
xEMU	Exploration Extravehicular Mobility Unit

2. Reading the LMEEM File

To accommodate the needs of Bumper, LMEEM outputs particle flux and other data in the form of an American Standard Code for Information Interchange (ASCII) text file. When reading this file, Bumper uses a combination of keywords and reading pre-defined character positions, thus data within this file must conform to a set structure.

The greatest flexibility is allowed in the header, an example of which is shown in Figure 2-1. The header, of arbitrary length, is defined by lines beginning with the number/pound/hash sign (#). Any number of lines may be added to the header, and Bumper will read past them unaffected. The LMEEM version number is shown in the figure, and additional information regarding the specifics of the file may also be included if the user desires.

```
# LMEEM Version af88221, Lunar Meteoroid Engineering Model
# Density: 3.1 g/cc
# Velocity: 0.175072     0.460514     1.138510     3.000000     4.200000
# Number Flux [#/m2/yr]
```

Figure 2-1 Example LMEEM Environment File Header

The two specific header lines shown in the figure above that Bumper does read are those defining the density and velocities of the particles. These two lines may appear anywhere in the header and in any order.

Bumper assumes that all particles in the LMEEM file have a single constant density, which Bumper reads from the header. Bumper searches the header for the keyword "Density" and extracts the decimal number (assuming units of g/cm^3) that follows. The value in this example, 3.1 g/cm^3, comes from Table 3.4.2.3-1 of Revision I of the Cross-Program DSNE [2]. This is expected to be the standard particle density for the lunar meteoroid ejecta environment in Revision J of the DSNE. Revision I cites different values based on lunar surface location, thus the particle density may be varied in the future. Bumper will read and use the particle density value in the file, however, only one value per file is currently permitted—a distribution of densities is not presently supported in Bumper for lunar ejecta.

Ejecta particles are launched at a range of velocities, from near-zero to beyond the lunar escape velocity of about 2.4 km/s. Bumper requires this range of velocities to be discretized into bins for processing. The Natural Environments Branch selected five bins for their initial LMEEM output files with guidance from the HVIT team (may vary in the future):

1. 0.1 km/s to 0.3 km/s
2. 0.3 km/s to 1.0 km/s
3. 1.0 km/s to 2.4 km/s
4. 2.4 km/s to 3.6 km/s
5. 3.6 km/s to 4.8 km/s

Bumper must assign each of these bins a single nominal velocity to use in computing the size of particle that can penetrate a shield. Those velocities must be provided in the header. Bumper searches the header for the keyword "Velocity" and extracts the decimal numbers (assuming units of km/s) that follow. The number of values in this line determines the number of velocity bins Bumper will expect throughout the remainder of the file. Up to ten values/bins may be provided, and the ensuing flux tables must all contain this same number of velocity bin columns. For the entirety of the file, Bumper will assign particles in each bin the associated nominal velocity read from the header's velocity line.

Particle velocity decreases with increasing size, as will be discussed further in later paragraphs, however, Bumper requires a single set of nominal velocities across all sizes. This single set of velocities is assigned via the header line. The example values in the figure above are the average velocities for $10^{-1.5}$ g particles (about a 2.7 mm sphere

at 3.1 g/cm^3) in the ensuing initial data file. This particle size was selected to represent the whole environment because it was deemed the best representation for particles that penetrate a generic Whipple shield. This logic is useful in selecting nominal velocity values to provide to Bumper through the header line in the absence of a compelling alternative, however, users are encouraged to select the velocities associated with whatever particle size is most critical to their specific spacecraft shielding.

The Bumper Response module calculates the particle size that just cases a shield to fail across a range of impact conditions. This module requires that the LMEEM file be specified so that it can read the density and velocities for use in developing its table of critical diameters. Bumper's Shield module uses this table in conjunction with flux values from the LMEEM file to compute risk. A single response file output (*.rsp) may be used in the Shield module in conjunction with different LMEEM files with different flux values, provided the particle density and nominal (header) velocities are identical. If LMEEM files use a different density or nominal velocities in their headers, then the Response module must be run separately for each LMEEM file.

Immediately after the last header line, as defined by beginning with "#," begins a data block for one increment of particle mass. Multiple blocks are used to provide data for a range of particle sizes. The initial LMEEM file uses 17 data blocks to detail the flux of particles ranging from one microgram to one hundred grams in half-decade intervals, however, these specifics are not required. An arbitrary number of data blocks may be provided, and Bumper will read blocks until the file ends. Bumper will read the particle mass associated with each block. The blocks must contain the lines shown in the example data block in Figure 2-2, and there must be exactly one blank line between each block.

```
Meteoroid Ejecta Mass >=   10^-6 g
 Speed Bin [m/s]    100 - 300   300 - 1000    1000-2400    2400-3600    3600-4800
 Elevation [deg] Speed Average [km/s]
PHI1 PHI2 PHIavg     0.184381     0.571955     1.551452     2.914856     4.126257
 -90  -80 -82.93 1.881316e-04 1.524981e-04 6.389583e-05 1.812096e-05 8.366369e-06
 -80  -70 -74.21 7.507099e-03 5.918393e-03 2.544112e-03 7.130276e-04 3.338226e-04
 -70  -60 -64.54 1.951937e-02 1.577366e-02 6.701586e-03 1.844939e-03 8.302170e-04
 -60  -50 -54.69 4.645156e-02 3.632598e-02 1.604136e-02 4.334148e-03 2.026947e-03
 -50  -40 -44.78 8.655783e-02 6.931975e-02 2.995122e-02 8.003225e-03 3.685105e-03
 -40  -30 -34.85 1.782930e-01 1.408085e-01 6.098200e-02 1.625529e-02 7.600915e-03
 -30  -20 -24.90 1.401961e-01 1.119278e-01 4.755482e-02 1.318926e-02 5.997585e-03
 -20  -10 -14.94 4.321013e-01 3.460033e-01 1.505490e-01 4.120061e-02 1.913988e-02
 -10    0  -4.98 3.075640e+00 3.614212e+00 2.148410e+00 5.590048e-01 2.509167e-01
   0   10   4.98 2.756279e+00 2.985610e+00 1.864028e+00 0.000000e+00 0.000000e+00
  10   20  14.94 7.107047e-01 5.732394e-01 2.259148e-01 0.000000e+00 0.000000e+00
  20   30  24.90 3.717665e-01 3.180463e-01 1.168219e-01 0.000000e+00 0.000000e+00
  30   40  34.85 2.197952e-01 1.949765e-01 6.884416e-02 0.000000e+00 0.000000e+00
  40   50  44.78 1.344563e-01 1.192000e-01 4.228538e-02 0.000000e+00 0.000000e+00
  50   60  54.69 7.605553e-02 6.775691e-02 2.519343e-02 0.000000e+00 0.000000e+00
  60   70  64.54 3.861011e-02 3.351178e-02 1.264196e-02 0.000000e+00 0.000000e+00
  70   80  74.21 1.482199e-02 1.186895e-02 4.901964e-03 0.000000e+00 0.000000e+00
  80   90  82.93 2.060226e-03 1.712756e-03 8.487701e-04 0.000000e+00 0.000000e+00
```

Figure 2-2 Example LMEEM Environment File Data Block

The first line defines the particle mass for that block. Bumper reads the mass (in grams) as the power of ten that begins with character number 29 in the line, using the format "10^" followed by the decimal number exponent. The next two lines define the speed bin limits and data labels; Bumper does not read these lines. The fourth line provides column headers for the ensuing table, and Bumper does not read this line either.

In the fourth line, the decimal value heading each of the flux data columns is the average velocity (in km/s) of the particles in that velocity bin at the defined size. The average velocity is a function of the particle size, with larger particles typically having lower ejection speeds. Bumper requires each velocity bin to have a single nominal velocity across all sizes to maintain consistency in its calculation of the particle size that penetrates a shield. Therefore, a single set of nominal velocities is provided to Bumper in the header as described above, and Bumper does not read the velocity values in the data blocks.

The remaining lines in the block define the elevation angle bins for which flux data is provided and provide that flux data for each velocity bin.

The first three fields define the elevation angle bins. Each bin is assigned a starting and ending angle, each using five characters, then the average elevation angle using the next seven characters. This average angle is the only angle of the three that Bumper reads. This angle is the elevation value for discrete three-dimensional threat directions that will be more fully defined in Section 3.2. A value of -90° indicates particles ascending from directly below the spacecraft that can strike a spacecraft's underside, a value of 0° indicates particles traveling parallel to the horizon, and a value on +90° indicates particles descending from directly above the spacecraft that can strike a spacecraft's top surface. The environment is agnostic to the azimuth component of directionality, as will be discussed in Section 3.2, thus the flux values are the total flux at that elevation from a full circle around the spacecraft isotropically. The 10° wide elevation bins shown in the example are the current LMEEM standard, however, Bumper is capable of reading other elevation layouts that follow the requisite character format. Bumper will detect that the block has ended via a blank line, thus the number of elevation bins is arbitrary. The elevation angles must be identical across all particle size blocks. The average elevation angle shown in the example is determined by averaging the sine of the starting and ending elevation for each block. This is also the current LMEEM standard, however, Bumper is capable of reading any value entered.

The Bumper Geometry module creates a table of environment threat-spacecraft FEM element combinations for use in risk calculations in the Shield module. The Geometry module requires that the LMEEM file be specified so that it can read the elevation angles for use in developing this threat-spacecraft table. A single geometry file output (*.gem) may be used in the Shield module in conjunction different LMEEM files with different flux values, provided the elevation angles are identical. If LMEEM files use different elevation angles, then the Geometry module must be run separately for each LMEEM file.

To the right of the elevation data is the flux data for that size and elevation in each bin. Bumper reads the flux values in 13-character increments, starting with character number 18. The number of flux values in each row must match the number of velocity bins defined in the header.

2.1. Bumper Analysis with LMEEM

When running Bumper, LMEEM behaves in the same manner as all other environments in all general respects. See the Bumper 3 Software User Manual [3] for more details on nominal Bumper usage. This section supplements the User Manual with discussion of some specific points of interest when using LMEEM.

When Bumper goes to read the LMEEM input text file, it will look for the file in a directory prescribed by the Runtime Control file. Use the command "LMEEMEJECTADIR" followed by a path to the desired directory to set the LMEEM directory.

A Finite Element Model (FEM) of the spacecraft is required for all Bumper analyses. The same FEM used with orbital debris and micrometeoroid environments can also be used with LMEEM. A unique consideration with LMEEM is the orientation of the FEM. Like with SP-8013, LMEEM uses a lunar surface-based coordinate system in which the +Z axis is the zenith direction—it points to space. Because the LMEEM environment is agnostic to the azimuth of threat directions, the X and Y axis are arbitrary. The FEM must be oriented such that the spacecraft model relative to the coordinate system accurately reflects this pointing. The Geometry module of Bumper provides an opportunity to rotate the FEM to accomplish this.

When running the Response module, it is important to ensure that the Ballistic Limit Equation (BLE) chosen accurately calculates critical particle sizes for velocities on the order of 0.175 km/s. This is substantially slower than

the hypervelocity impact data BLEs are usually derived from. It may be necessary to conduct lower speed impact testing to validate that a BLE is accurate in this velocity range. Specialized BLEs focused solely on this velocity range may be desired for critical items; this must be worked with the HVIT Group for inclusion into Bumper.

3. Validation of Bumper Calculations

The validation process for implementation of LMEEM into Bumper centered on two questions:

- Is Bumper performing the right process to match the intent?
- Is Bumper performing that process correctly?

3.1. Basic Intent

Bumper requires incoming threats to be defined in three-dimensional space to interact with a three-dimensional finite element model of the spacecraft. However, LMEEM flux is only defined relative to an elevation angle, while considering the flux to be isotropic relative to azimuth.

To bridge this gap, Bumper maps LMEEM flux onto a sphere composed of discrete patches, commonly referred to as an igloo due to the appearance of the patches resembling the blocks of an igloo. Figure 3-1 shows an image of the igloo created within Bumper for LMEEM.

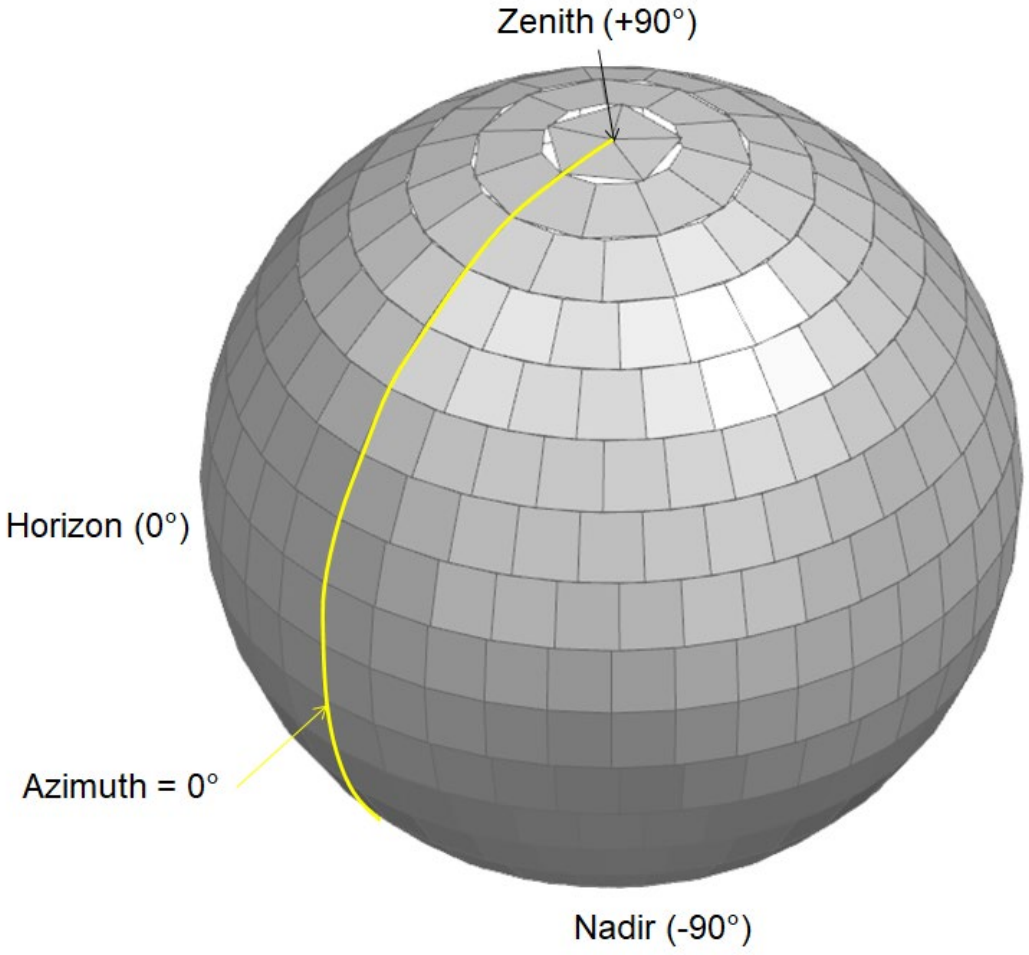


Figure 3-1 LMEEM Igloo

The elevation bins are defined by the LMEEM file as previously discussed; the default bins are 10° wide. The azimuth bins vary in angular width at each elevation row to achieve a near-constant solid angle for all patches around the sphere.

The algorithm Bumper uses to define the azimuth bins begins by setting an angular width based on the most polar elevation bin being divided into five azimuth bins:

$$Polar\ Angular\ Width = \frac{2\pi * \cos(elevation\ at\ most\ polar\ bin)}{5}$$

The number of azimuth bins at all other elevations is set based on this width:

$$Number\ of\ Bins = Floor\left(\frac{2\pi * \cos(elevation)}{Polar\ Angular\ Width}\right)$$

At each elevation, the requisite number of azimuth bins of equal width are created, starting at the azimuth = 0° line. The flux of particles at that elevation is divided equally among the azimuth bins.

When a Bumper analysis is performed, each element of the spacecraft finite element model is placed at the center of this igloo and subjected to threats originating from each patch in the sky-sphere. The elevation angle of a given threat is the average elevation read from the LMEEM file. The azimuth angle of a given threat is the average of the starting and ending azimuth angles for that patch as defined by the algorithm above.

To validate that this igloo process correctly captures the intent of the LMEEM file, which is agnostic to azimuth, a comparison was made between a Bumper impact assessment and a hand calculation.

A simple cube with one meter edge lengths was used to represent the spacecraft. The analysis and calculation were both performed using an LMEEM environment in which the flux value for every size, elevation, and velocity was fixed to 0.00002 particles per square meter per year. Defining the flux to be constant avoided calculations extraneous to the goal of evaluating the validity of the igloo.

In the hand calculation, the top, side, and bottom were each considered. Across all elevations, the unique impact angle to the cube face was calculated, and the flux was multiplied by the cosine of this angle. For the top and bottom faces, all elevations that only view the backside of the face were excluded. For the top and bottom faces, azimuth does not change the impact angle and did not need to be considered further, however, for the cube side, azimuth angle does need to be accounted for. The flux needs to be multiplied by the cosine of the azimuth angle between the threat and surface normal, with those threats that only view the backside of the face excluded. The average cosine across all azimuth angles was calculated to be 0.3183, indicated by the dashed line in Figure 3-2, which graphs the cosine of azimuth angles compared to a 0° face normal direction.

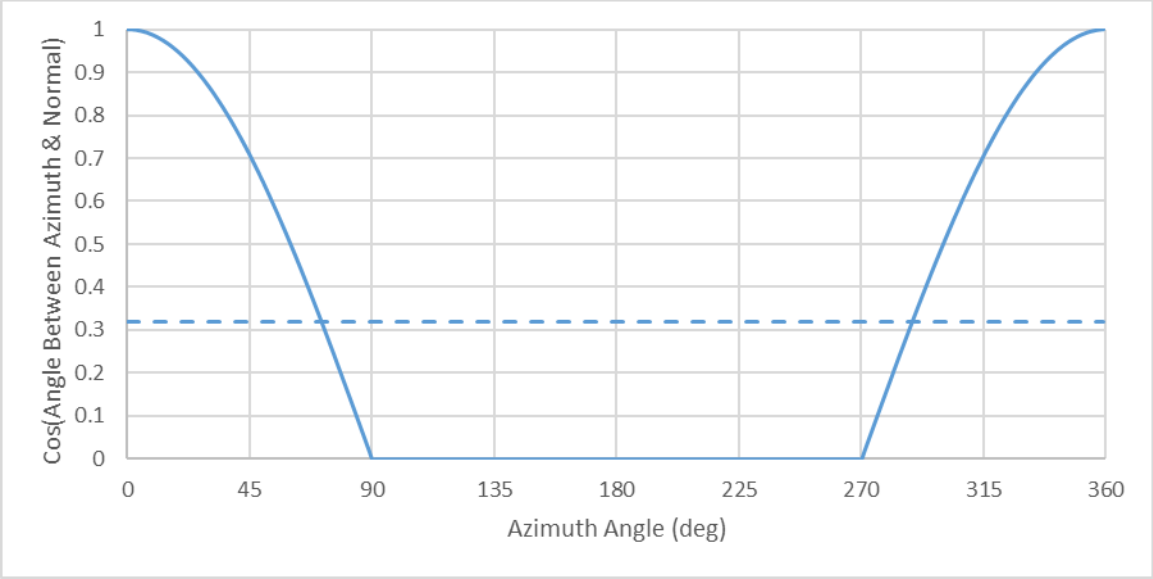


Figure 3-2 Average Azimuth Cosine

This impact angle-factored flux was multiplied by five to count the five independent velocity bins and was multiplied by the 1 m^2 area and 1-year duration to arrive at a number of impacts. The elevation cosine values and numbers of impacts are given in Table 3-1. Summing the number of impacts across elevations gave the total number of impacts to each face, shown at the bottom. This hand calculation was compared to the output of a Bumper analysis that assessed the number of impacts on a cube using an LMEEM environment file modified to have the same constant flux. As shown at the bottom of the table, the hand calculation and Bumper output match to within a small tolerance, indicating that Bumper's igloo is replicating the intent of LMEEM.

Table 3-1 Basic Intent Hand Calculation Comparison

Elevation	Cosine Due to Elevation			Impacts		
(Deg)	Side	Top	Bottom	Side	Top	Bottom
-82.93	0.1231	0.0000	0.9924	2.3506E-06	0.0000E+00	5.9544E-05
-74.21	0.2721	0.0000	0.9623	5.1968E-06	0.0000E+00	5.7736E-05
-64.54	0.4299	0.0000	0.9029	8.2099E-06	0.0000E+00	5.4173E-05
-54.69	0.5780	0.0000	0.8160	1.1039E-05	0.0000E+00	4.8962E-05
-44.78	0.7098	0.0000	0.7044	1.3556E-05	0.0000E+00	4.2263E-05
-34.85	0.8207	0.0000	0.5714	1.5673E-05	0.0000E+00	3.4286E-05
-24.9	0.9070	0.0000	0.4210	1.7323E-05	0.0000E+00	2.5262E-05
-14.94	0.9662	0.0000	0.2578	1.8453E-05	0.0000E+00	1.5468E-05
-4.98	0.9962	0.0000	0.0868	1.9026E-05	0.0000E+00	5.2085E-06
4.98	0.9962	0.0868	0.0000	1.9026E-05	5.2085E-06	0.0000E+00
14.94	0.9662	0.2578	0.0000	1.8453E-05	1.5468E-05	0.0000E+00
24.9	0.9070	0.4210	0.0000	1.7323E-05	2.5262E-05	0.0000E+00
34.85	0.8207	0.5714	0.0000	1.5673E-05	3.4286E-05	0.0000E+00
44.78	0.7098	0.7044	0.0000	1.3556E-05	4.2263E-05	0.0000E+00
54.69	0.5780	0.8160	0.0000	1.1039E-05	4.8962E-05	0.0000E+00
64.54	0.4299	0.9029	0.0000	8.2099E-06	5.4173E-05	0.0000E+00
74.21	0.2721	0.9623	0.0000	5.1968E-06	5.7736E-05	0.0000E+00
82.93	0.1231	0.9924	0.0000	2.3506E-06	5.9544E-05	0.0000E+00
			Hand Calculation:	3.6942E-04	5.7151E-04	5.7151E-04
			Bumper:	3.6952E-04	5.7151E-04	5.7151E-04
			Difference:	0.0262%	0.0000%	0.0000%

Elevation

Complement of Elevation

Backside Threat

3.2. Bumper Calculation Process

To further verify Bumper's calculation process, including the mathematics of the specific threat directions generated by the igloo, a more detailed hand calculation was performed for comparison to the same Bumper output.

Each igloo patch's threat direction was identified and its impact angle to each face of the cube was calculated. The cosine of each impact angle was recorded, which was set to zero for threats that only view the backside of the face. The number of impacts from each patch striking each face was calculated by multiplying the same constant flux value of 0.00002 particle per m^2 per year by the cosine of the impact angle and dividing this by the number of patches at that elevation angle. This value was multiplied by the 1 m^2 area and 1-year duration to arrive at a number of impacts. The number of impacts for each face was summed across all patches to give the total number of impacts to each face reported in Table 3-2.

Table 3-2 Igloo Calculation Hand Calculation Comparison

	Ram	Wake	Port	Starboard	Zenith	Nadir
Hand Calculation:	3.6996E-04	3.6996E-04	3.6908E-04	3.6908E-04	5.7151E-04	5.7151E-04
Bumper:	3.6996E-04	3.6996E-04	3.6908E-04	3.6908E-04	5.7151E-04	5.7151E-04
Difference:	0.0000%	0.0000%	-0.0001%	-0.0001%	0.0000%	0.0000%

The table compares these results to the Bumper output, which match to within the significant figures output by Bumper. This verifies that Bumper's igloo calculations are being performed as intended.

A final layer of complexity was added to the hand calculation comparison: determining and using flux as a non-constant function of critical diameter. For this check, the above process was repeated with one change. A simple power function was used to define flux as a function of mass. For every elevation angle and velocity, the flux as a function of mass was defined as:

$$Flux\left(\frac{particles}{m^2 * year}\right) = 0.0000001 * mass\ (g)^{-1}$$

This formula allowed for flux to vary with mass in a way that was manageable in a hand calculation.

Each face of the cube was defined as having a Whipple shield composed of a 0.1 cm Al6061-T6 bumper wall, a 10 cm standoff, and a 0.3 cm Al6061-T6 rear wall. The New Non-Optimum BLE [4] was used to determine the critical particle diameter for each of the five velocities shown in the example above and impact angles in 5° increments for particles with a density of 2.5 g/cm^3, as was expected to be the standard at the time the check was performed.

For each patch-face combination and each velocity, the critical diameter was determined from the ballistic limit (linearly interpolating on the geometrically-defined impact angle), and the flux of particles was determined from the mass of the spherical critical particle using the formula above. This critical flux was then used in the same number of impact calculation described previously.

A corresponding Bumper analysis was performed using an LMEEM file modified to reflect the flux-mass relationship formulated above. The hand-calculated impacts and Bumper output are compared in Table 3-3.

Table 3-3 Flux Calculation Hand Calculation Comparison

	Ram	Wake	Port	Starboard	Zenith	Nadir
Hand Calculation:	1.5617E-05	1.5611E-05	1.5613E-05	1.5613E-05	4.1044E-05	4.1044E-05
Bumper:	1.5618E-05	1.5611E-05	1.5614E-05	1.5614E-05	4.1046E-05	4.1046E-05
Difference:	0.0030%	0.0026%	0.0028%	0.0028%	0.0034%	0.0034%

The hand calculation matches the Bumper output to within two digits of the last significant figure output by Bumper.

During this final check, the interpolation scheme used to determine the flux from the mass in Bumper was graphed and visually inspected to determine that it gave sensible results, specifically, a straight line in log-log space.

These checks investigated each step in the calculation for overall sensibility. Matching Bumper results to hand calculations that methodically step through the process verifies that both Bumper is performing the calculations that it should, and it is performing these calculations correctly.

4. Initial LMEEM Environment File

An initial LMEEM flux file was provided by the Natural Environments Branch during April, 2024. The definitive version of this LMEEM text file is named "primary_LMEEM_DSNE_Environment_V0.1.4.lmeem" [5].

This file represents the ejecta environment for any latitude on the Moon. Various latitude locations were considered, and the worst-case flux across these latitudes was included for each elevation/velocity case independently. The worst-case longitude of 270 degrees East (the western limb) was used in all the previous cases. Similarly, heights above the surface ranging from 7 m to 50 m were considered and the worst-case flux for each elevation/velocity case was found and included in the file. The meteoroid environment used to determine the lunar impacts from which ejecta is launched assumed the average incoming meteoroid fluxes seen over 19 years at various locations over the surface of the Moon.

Figure 4-1 graphs the particle flux as a function of mass for LMEEM in blue and SP-8013 in orange. The black dots are summation of flux across elevation and velocity for each mass, with the blue line being the interpolated values between these fiducial points. The two smallest-mass points are used to extrapolate to even smaller particle sizes, which are necessary in some lunar dust-focused analyses. Sizes larger than 100 g are not generally necessary for accurate risk assessments, and a simple cut-off is used such that the cumulative flux for any larger particle is fixed at the cumulative flux for 100 g particles. The SP-8013 flux is the value calculated by the equation in Section 3.2.3.1 of that document.

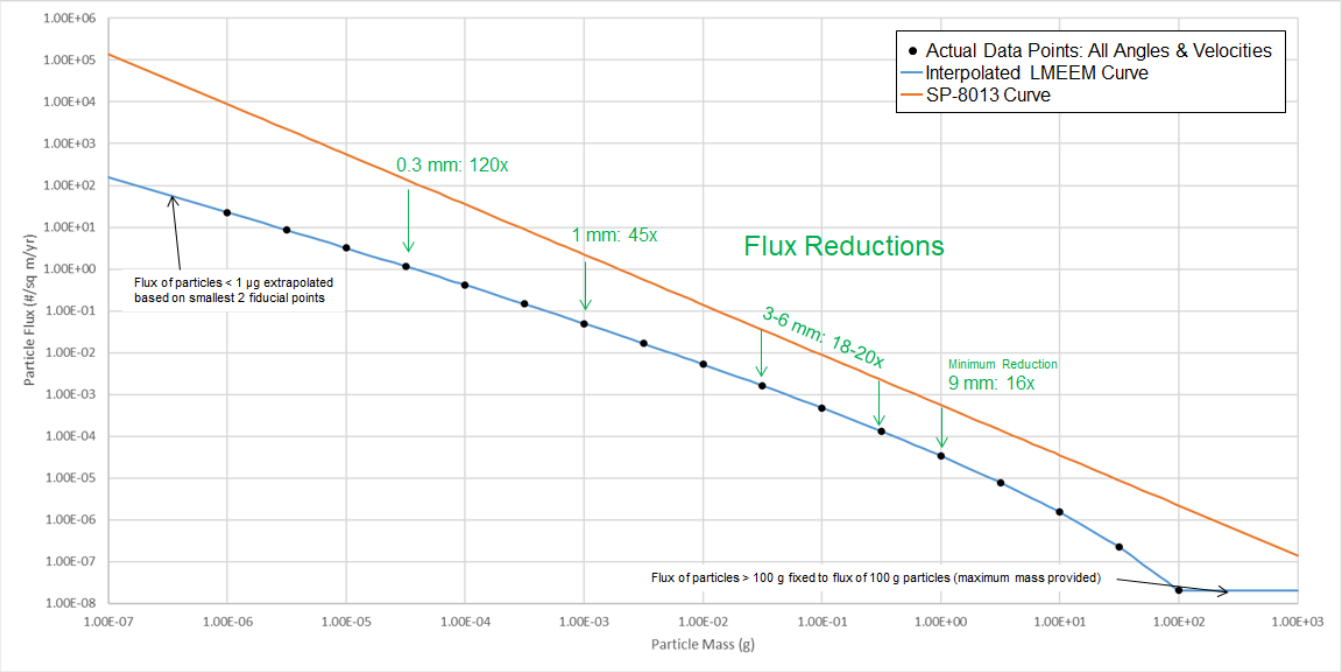


Figure 4-1 LMEEM Flux as a Function of Mass (Compared to SP-8013)

The SP-8013 flux is assumed to be the flux experienced by a specifically oriented flat plate, however, the LMEEM flux is that experienced by a sphere. While this difference in methodology disrupts the direct comparison being made, it is valid to note that LMEEM flux is at least an order of magnitude lower than SP-8013 flux for all masses, and two orders of magnitude lower for dust particles.

Figure 4-2 examines the flux directionality. The igloo previously shown was created as a finite element model, and each patch was colored based on its flux of 0.1 g particles—equivalent to a 3.95 mm sphere. As indicated, blue represents low flux and red represents high flux. The consistency in color across each horizontal band is due to LMEEM being agnostic to azimuth and the flux distributed evenly around the circumference.

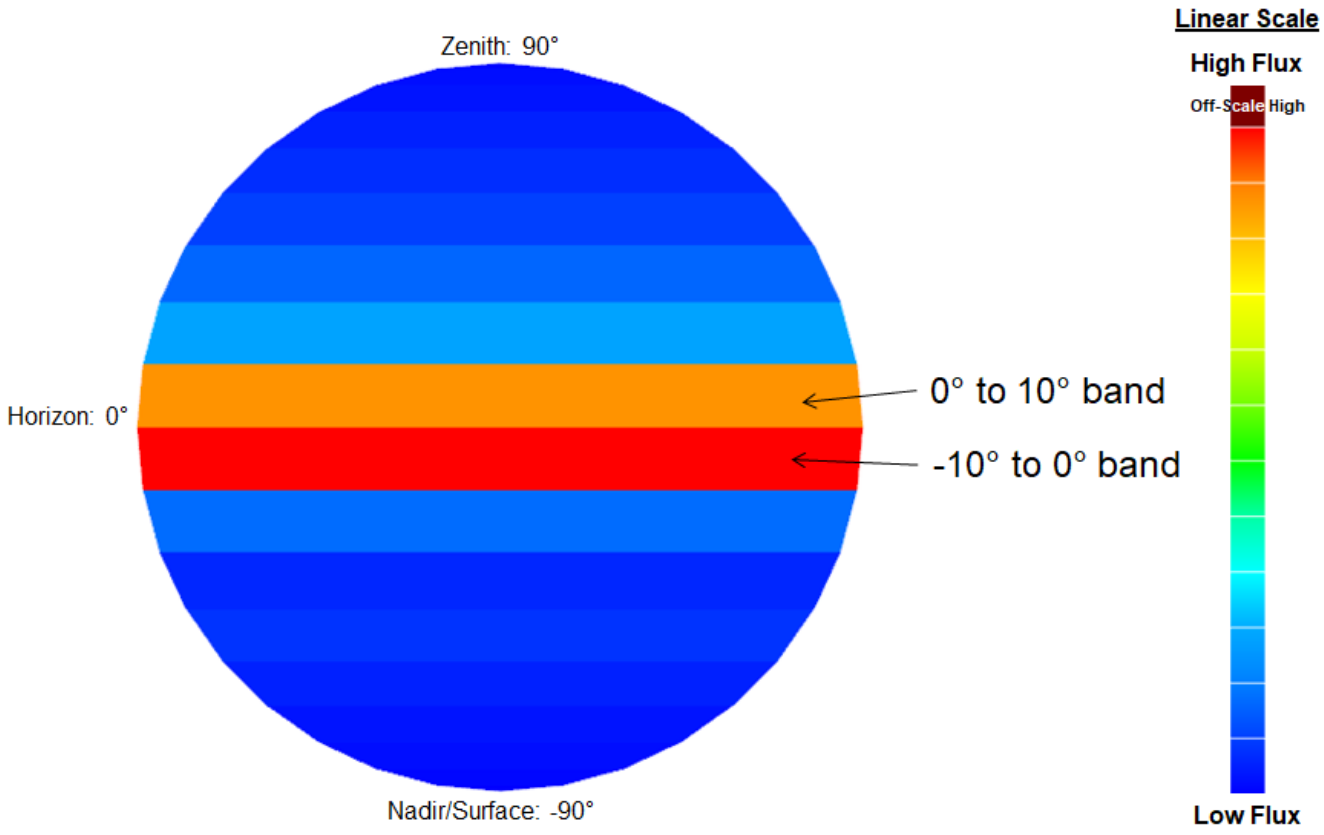


Figure 4-2 LMEEM Flux Directionality

The figure shows that the majority of flux is close to horizontal, falling into one of the two bins that straddle the horizon. Figure 4-3 breaks the flux down into ascending (near field, blue) and descending (far field, red). Using the horizon as the dividing line, as indicated on the right side of the inset, ascending and descending fluxes (solid lines) are close to even across all sizes, with ascending flux being slightly higher for the smallest size and descending flux being higher for the largest sizes. However, if the flux were divided into three parts (dashed lines), with ascending and descending joined by a middle section (purple) composed of ±10° from the horizon, the middle section is the dominant contributor to flux, ranging from 65% to 75% of the total, and descending flux always exceeds ascending flux.

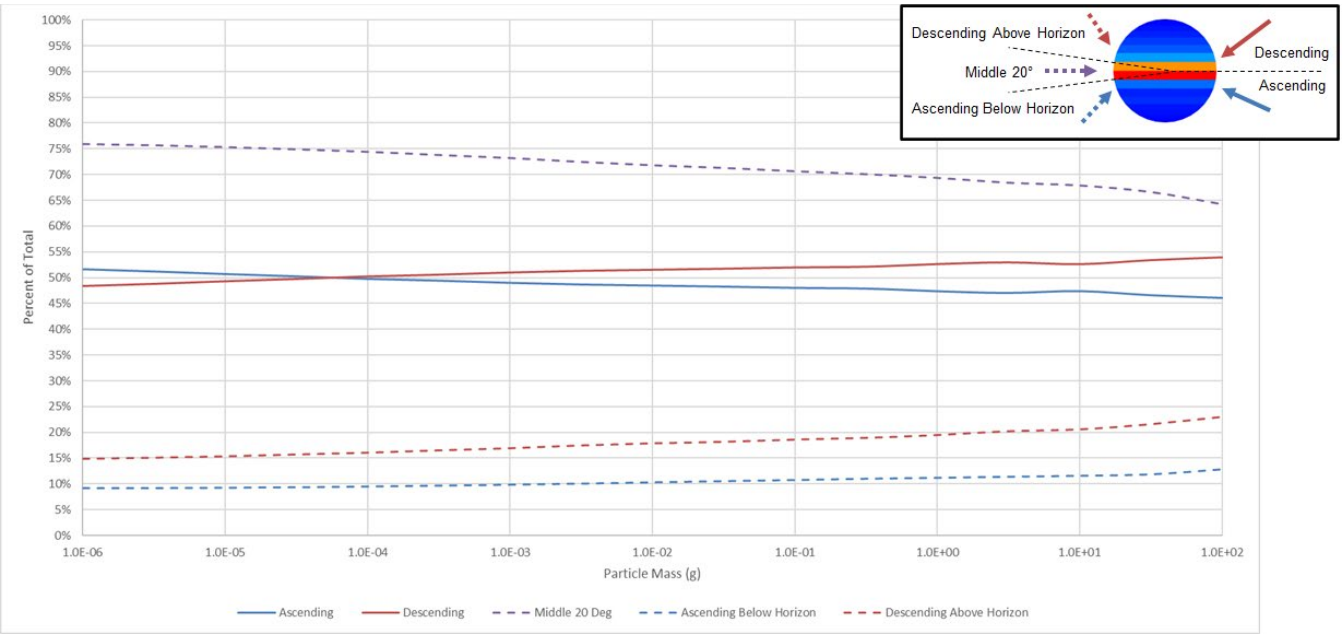


Figure 4-3 LMEEM Flux Ascending vs. Descending

This directionality contrasts with SP-8013, which is implemented in Bumper such that all flux descends from angles between 40° and 50° above the horizon.

Only particles with a mass of 0.01 g (~2 mm diameter) or less exceed escape velocity. The portion exceeding escape velocity is always less than five percent. Particles exceeding escape velocity are always ascending, as such a particle will, by definition, not descend back to the Moon.

4.1. Current & Future LMEEM Features

The particle density in the initial file is 3.1 g/cm^3. Variation in particle density may be considered in the future evolution of LMEEM.

The near field portion of the environment is the portion with an upward trajectory (elevation < 0° = ascending) as it ejects from the excavating crater, while the far field portion of the environment is the portion with a downward trajectory (elevation > 0° = descending) as it falls back to the Moon. The dividing line between near and far field is reaching apolune. Both of these categories are included in a single environment. While not expressly labeled as near or far field, they can be differentiated by elevation as noted.

Velocity greater than escape velocity is included and is only present for the near field ejecta.

The initial file is time-agnostic, including ejecta from sporadic background meteoroids only. Time specific analyses, including effects of meteoroid showers, is an important long-term goal for Natural Environments Branch customers.

The Lunar meteoroid ejecta environment from LMEEM can be created at any position on or above the Moon for any cylindrically shaped asset. Currently the surface properties in LMEEM are broken down into two categories, highlands and mare.

The initial file is generic relating to height off the surface. Flux as a function of height along the asset may be included in later LMEEM development.

5. Comparison between SP-8013 & LMEEM

A series of comparisons between risk with SP-8013 and risk with LMEEM were performed to understand how risk will change with the new model.

Two basic geometry models were assessed in each lunar ejecta environment, a cube with 1 m^2 faces and a sphere with a cross sectional area of 1 m^2. Each model was assessed for penetrations of a Whipple shield composed of a 0.1 cm Al6061-T6 bumper wall, a 10 cm standoff, and a 0.3 cm Al6061-T6 rear wall of for impacts by a 6 mm particle, which approximates the critical diameter for this shield for 0.5 m/s normal impacts.

Table 5-1 shows the risk results for the cube (broken down by face and the total) and sphere, for both impacts and penetrations, for each environment, along with the difference that manifests going from SP-8013 to the LMEEM model.

Table 5-1 Basic Ejecta Risk Comparison

	6 mm Impacts			Whipple Penetrations		
	SP-8013	LMEEM	Difference	SP-8013	LMEEM	Difference
Horizontal +X	8.0737E-04	3.5832E-05	-96%	3.3725E-06	2.3812E-06	-29%
Horizontal -X	8.0783E-04	3.5832E-05	-96%	3.3749E-06	2.3804E-06	-29%
Horizontal +Y	8.0745E-04	3.5824E-05	-96%	3.3745E-06	2.3807E-06	-29%
Horizontal -Y	8.0739E-04	3.5824E-05	-96%	3.3744E-06	2.3807E-06	-29%
Zenith	2.5274E-03	1.3061E-05	-99%	1.4266E-05	1.2934E-07	-99%
Nadir	0.0000E+00	9.3714E-06	-	0.0000E+00	7.0221E-08	-
Cube Total	5.7574E-03	1.6574E-04	-97%	2.7762E-05	9.7226E-06	-65%
Sphere	3.5818E-03	1.1736E-04	-97%	3.8382E-05	4.5137E-06	-88%

Switching from SP-8013 to LMEEM results in a 97% reduction in impacts to the sphere and cube, including reductions of at least 96% to every face of the cube except the nadir. The number of penetrations of the Whipple-shielded sphere was reduced by 88%, while the cube penetrations were reduced by 65%. This included a 99% reduction to penetrations of the Zenith face and a much lower 29% reduction to each horizontal face. This difference in effect is due to directionality. SP-8013 flux is exclusively descending at a steep angle such that it strikes the horizontal and zenith faces at roughly 45° off from the face normal directions. The LMEEM flux, as seen in Section 4, is largely aligned with the horizon. This means that strikes to the horizontal faces are nearly normal to the surface, which results in a smaller critical particle size than SP-8013's oblique strikes, partially negating LMEEM's broad reduction in flux as a function of mass. Strikes to the zenith face are of a nearly glancing incidence, resulting in larger critical particle sizes and increased risk reduction compared to LMEEM's reduction in flux as a function of mass alone. The reason the risk reduction to a Whipple-shielded cube is lower than the risk reduction to a similar sphere is because the cube's four horizontal faces and one zenith face emphasizes LMEEM's horizontal directionality effect compared to the smoothly curve sphere that points in all directions equally.

The nadir face points at the lunar surface from an unspecified height above the surface of the Moon; this height is between 7 m and 50 m, as discussed in Section 4. This face is not exposed to any SP-8013 threat directions, and thus carries no risk in that analysis, however, ascending particles do exist in LMEEM, and they can strike this surface. The nadir face represents 6% of the cube impact risk, similar to the zenith face (8%), and almost four times lower than the horizontal faces. Assessing penetrations of a Whipple shield reduce the nadir face's contribution to 1% of risk—again, similar to the zenith face—due to the aforementioned LMEEM horizontal flux directionality effect.

Table 5-2 breaks down the impacts and penetrations to the sphere by velocity. Impacts are strongly driven by the slowest velocity (0.175 km/s), which accounts for 88% of the total. The two faster bins below escape velocity contribute risk in amounts that rapidly decrease with velocity due to the flux decreasing with velocity in the same fashion. Penetrations are also driven by slowest velocity, but to a lesser degree, accounting for only 58% of the total. The second slowest velocity (0.46 km/s) contributes far more to penetrations (40%) than to impacts (12%), as does the highest sub-escape velocity (1.14 km/s). This shift in risk toward higher velocity, when comparing penetrations to impacts, is due to higher velocities resulting in smaller critical particle sizes with correspondingly greater flux. Only particles up to 0.01 g in mass (~2 mm in diameter) exceed escape velocity, thus this velocity regime does not contribute any risk to this assessment of 6 mm impacts or penetrations of a Whipple shield for which the critical particle size is always greater than 0.01 g.

Table 5-2 LMEEM Risk by Velocity

	6 mm Impacts	Whipple Penetrations
0.175 km/s	88%	58%
0.46 km/s	12%	41%
1.14 km/s	0.0015%	1%
3 km/s	0%	0%
4.2 km/s	0%	0%

Directionality can be further investigated using a contour plot, in which each element of a geometry model is colored according to its risk (mean number of penetrations) per unit area. In the figures below, the sphere from the previous assessment is depicted in a contour plot in which blue represents low risk and red represents high risk. In this view, the zenith direction is up and nadir down, with the horizon being a plane stretching left and right. The two spheres to the left of the thick black vertical line are graphed on the same scale for a direct comparison between SP-8013 (left) and LMEEM (center), however, in both cases, LMEEM risk is orders of magnitude lower than SP-8013 risk, thus, LMEEM risk contours are not visible at that scale. Therefore, the LMEEM risk is also graphed to the right on its own scale to resolve the risk contours. In all cases, the risk contours are consistent around each sphere in an azimuth direction, as both ejecta environments are agnostic to azimuth, and vary only in the elevation direction.

Figure 5-1 shows the contour plot for impacts of 6 mm particles. Both risk contours reflect directionality previously discussed. The SP-8013 risk is highest at the zenith pole and decreases as elevation progresses toward the nadir pole. The LMEEM risk is highest at the horizon and decreases as elevation moves toward each pole.

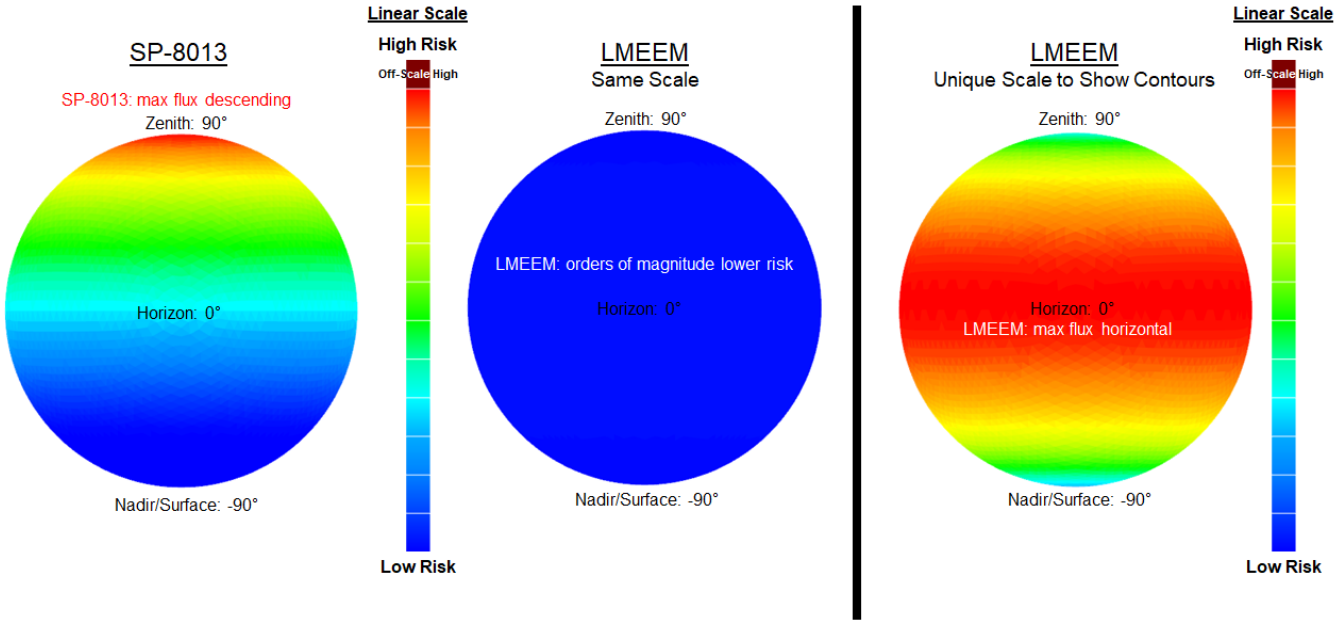


Figure 5-1 Ejecta Contour Comparison: 6 mm Impacts

Figure 5-2 shows the contour plot for penetrations of the Whipple shield described above. A penetration analysis focuses emphasis on normal impacts because BLEs tend toward smaller, higher-flux critical particles at lower impact angles. This narrows the color bands to regions corresponding to the highest-flux threat directions. For SP-8013, this resolves the actual ring of threats descending from between 40° and 50° above the horizon. For LMEEM, the red band tightens around the horizon.

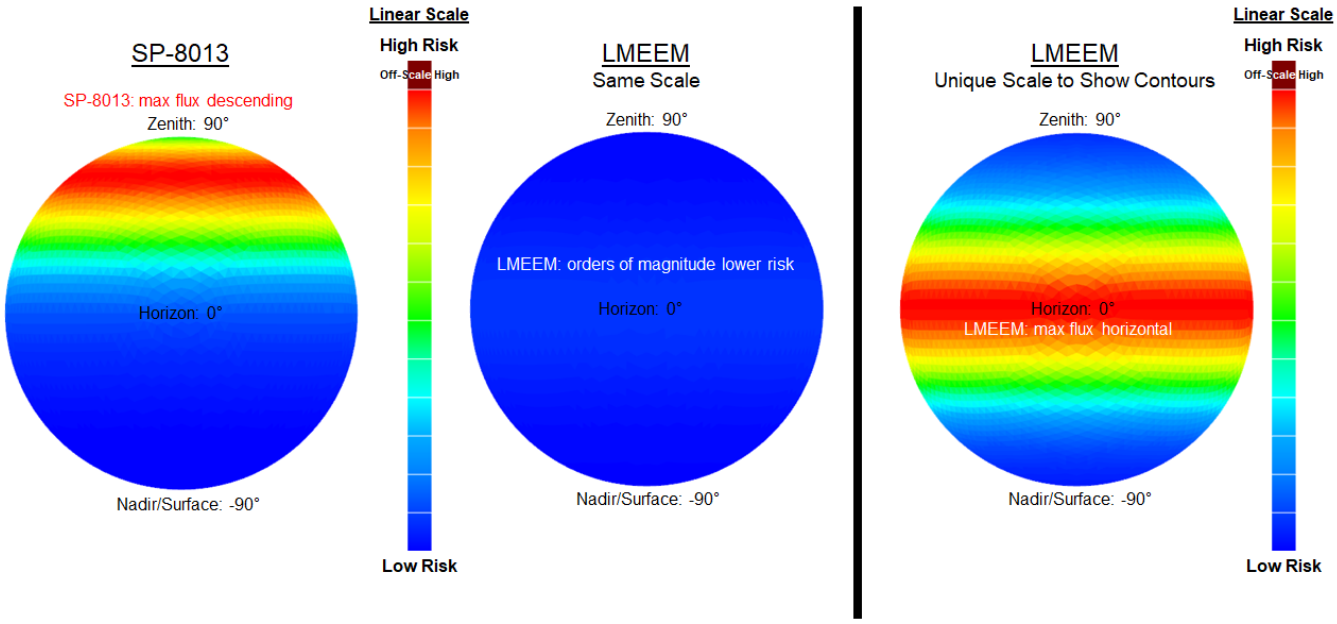


Figure 5-2 Ejecta Contour Comparison: Whipple Shield Penetrations

To extend the comparison from simple geometries to an actual spacecraft with realistic shielding, a lunar lander was assessed for ejecta risk using each environment model. The specific lander used will not be detailed due to design data sensitivity.

It was found that risk of a critical failure of the lander due to ejecta reduced by 75% with LMEEM compared to SP-8013. The SP-8013 ejecta risk was approximately 30% of the total MMOD risk while sitting on the surface of the Moon, contributing less than half as much risk as direct meteoroid strikes as assessed using the MEM 3 model, and ejecta was a negligible contributor to the overall lunar mission, which spent most of its time in orbit. Therefore, total MMOD risk with LMEEM will be lower than with SP-8013, perhaps by an amount on the order of 20% for time spent on the lunar surface.

Seven of the eleven spacecraft systems assessed saw risk reductions between 64% and 84%. These results correspond to the 65% penetration risk reduction of the cube shown above, skewed slightly toward the sphere's 88% penetration risk reduction, likely due to geometry that emphasizes horizontal sides like a cube, but with a degree of sphere-like rounding.

Four systems showed risk changes outside this range, all of which correspond to unique geometric features:

- An almost purely zenith-facing system saw an orders of magnitude risk reduction with LMEEM similar to the cube's zenith face.
- An almost purely nadir-facing system saw the appearance of some risk with LMEEM where there had been almost none with SP-8013, similar to the cube's nadir face.
- An almost purely horizontal-facing system saw lesser risk reduction with LMEEM than other systems saw, similar to the cube's horizontal faces compared to the cube's total.
- A system with large critical diameters had its risk driven by each environment model's unique large particle flux cut-off (3 cm for SP-8013 versus 100 g {~3.95 cm} for LMEEM), leading to much lower risk with LMEEM due to the cut-off particle size being larger.

To compare SP-8013 and LMEEM risk assessments when extremely small critical particles (relative to a well-shielded lander) are involved, a comparison analysis was performed using the Exploration Extravehicular Mobility Unit (xEMU) suit. The suit includes regions where particles on the order of 0.05 cm (0.16 mg at 2.5 g/cm^3 or 0.2 mg at 3.1 g/cm^3) can cause a failure.

Ejecta risk to the soft goods regions, including the arms, legs, and gloves was 2.9 times higher with LMEEM than with SP-8013, while for the hard goods regions of the torso, helmet, and backpack, LMEEM resulted in a 95% decrease in risk compared to SP-8013. Because soft goods drive the overall risk, the total xEMU suit ejecta risk increases with LMEEM by a factor of 2.9 over the SP-8013 ejecta risk.

Further investigation into the increase in risk to soft goods with LMEEM determined that the cause is a confluence of a change in velocity and the specific BLE used to assess soft goods.

As noted in the velocity breakdown above, risk from the LMEEM environment is dominated by the lowest velocity bin, and the same is true of SP-8013. For SP-8013, this lowest velocity is 0.1 km/s; for LMEEM, the lowest velocity is 0.175 km/s.

The critical particle size at 0.1 km/s and 2.5 g/cm^3 (used by SP-8013) is 26.5 g (2.7 cm diameter) for 45° impacts, which is a common impact angle for the descending SP-8013 flux to strike these horizontally oriented surfaces. At 0.175 km/s, 3.1 g/cm^3, and 0° impacts, as is common for LMEEM's horizontal threats, the critical particle size is 0.265 g (0.55 cm). The factor of five difference in diameter and two order of magnitude difference in mass reflects three differences: 1) LMEEM's greater particle density, 2) reduced impact angle with LMEEM, and 3) a slope in the ballistic limit curve at these velocities that is unusually close to vertical. The third item is the key differentiator between this analysis region that showed an increased risk with LMEEM and other analysis regions that exhibit only the first two items, such as horizontal cube faces, which still show a risk decrease with LMEEM.

The flux examination in Section 4 indicated that LMEEM flux is one order of magnitude lower than SP-8013 flux for a given mass. However, when the critical mass is reduced by two orders of magnitude when transitioning from SP-8013 to LMEEM, the flux of critical particles will be higher for LMEEM, resulting in higher risk.

Thus, while most comparisons showed that using LMEEM results in lower ejecta risk than SP-8013, at least one case has been identified where LMEEM results in higher risk due to the increase in the lowest velocity considered interacting with a BLE sensitive to that change.

6. Conclusion

The lunar ejecta environment, material launched from the surface as meteoroids strike the Moon, is an important factor to consider for spacecraft operations on the Moon's surface. The environment was first characterized by the paper NASA SP-8013 [1], and a new model, LMEEM, has been designed to improve the accuracy and detail of the lunar ejecta environment.

NASA's Bumper code for MMOD risk analysis has been modified to read ejecta flux and other data from text files output by LMEEM and to perform risk calculations for spacecraft on the lunar surface. See Section 2.1 for helpful information in performing Bumper analyses with the LMEEM environment model.

The implementation of code to read LMEEM files and perform risk calculations is considered validated. The checks detailed in Section 3.1 demonstrate that Bumper's coding reflects the design intent of the LMEEM environment, and the checks detailed in Section 3.2 demonstrate that Bumper's calculations are being performed correctly.

The initial LMEEM environment model, detailed in Section 4, contains particle flux values that are lower than those of SP-8013 for a given particle mass. For particles in the range most critical to effective shields, LMEEM flux is on the order of 20 times lower; for dust particles, LMEEM flux is on the order of 100 times lower.

The directionality of the LMEEM environment is different from SP-8013. The SP-8013 model only considers particles descending onto a spacecraft from above at angles between 40° and 50° above the horizon. While LMEEM includes particles striking the spacecraft from all elevations, the majority of LMEEM risk comes from particles traveling roughly parallel to the Moon's surface. Both models are agnostic to azimuth angle in the plane of the Moon's surface.

The majority of LMEEM risk comes from the lowest velocity bin, currently set at 0.175 km/s, for both shield penetrations and especially impacts. This is an increase in velocity from the 0.1 km/s value that represents the majority of SP-8013 risk. The vast majority of LMEEM risk comes from impacts slower than 0.5 km/s, however, particles exceeding escape velocity are also included. Only lightweight particles exceed escape velocity.

Section 5 compares risk assessments using SP-8013 and LMEEM. Assessments using simple geometry show a 97% reduction in particle impacts to both a cube and a sphere when using LMEEM compared to SP-8013; this is due to lower flux in the LMEEM environment. Penetrations of a Whipple shield are reduced by 65% for the cube and 88% for the sphere, with the difference in outcome being due to the change in directionality.

A comparison of analyses of a lunar lander showed a 75% reduction in ejecta risk with LMEEM compared to SP-8013. This translates into a total MMOD risk reduction of potentially 20% for a spacecraft on the surface of the Moon when also including direct strikes by micrometeoroids using the MEM 3 environment model. Detailed examination showed behavior similar to that outlined using simple geometry, including risk reductions due to lower flux with LMEEM that can be either moderated or enhanced by changes in directionality, depending on local geometry.

A comparison of analyses of a spacesuit identified a condition in which LMEEM can produce higher risk than SP-8013. This condition is a confluence of the increase in the dominant velocity from 0.1 km/s to 0.175 km/s and a BLE whose output is more strongly affected by that change than most BLEs due to the unusually steep slope of the ballistic limit curve in that velocity regime. This example emphasizes the importance of having accurate ballistic performance calculations at the relevant velocities for lunar ejecta, which may often require further impact testing.

7. References

1. B.G. Cour-Palais, et al., NASA SP-8013, “Meteoroid Environment Model – 1969 [Near Earth to Lunar Surface],” March 1969
2. SLS-SPEC-159 Revision I, “Cross-Program Design Specification for Natural Environments (DSNE),” October 2021
3. M. Bjorkman, NASA TM-2014-218559, “Bumper 3 Software User Manual,” October 2014
4. E.L. Christiansen, NASA TP-2003-210788, “Meteoroid/Debris Shielding,” August 2003
5. A. DeStefano, primary_LMEEM_DSNE_Environment_V0.1.4.lmeem, April 2024